FACTA UNIVERSITATIS
Series: **Electronics and Energetics** Vol. 38, Nº 3, September 2025, pp. 397 - 430
https://doi.org/10.2298/FUEE2503397G

Original scientific paper

PROBABILISTIC DISTRIBUTION SYSTEM PLANNING: INTEGRATING PV-BASED DG, DSTATCOM, AND RECONFIGURATION UNDER SOLAR IRRADIANCE AND LOAD UNCERTAINTIES

Pragya Guru[1], Nitin Malik[2], Sheila Mahapatra[3]

[1,2]The NorthCap University, Gurugram-122017, India
[3]Alliance University, Bangalore-562106, India

ORCID iDs:	Pragya Guru	https://orcid.org/0009-0009-5858-5463
	Nitin Malik	https://orcid.org/0000-0003-1484-9841
	Sheila Mahapatra	https://orcid.org/0000-0001-6502-0772

Abstract. *Recent technological developments in power distribution networks (PDN) have triggered significant interest regarding the optimal operation of power grids. Despite the high cost of power network development and installation, there is a significant opportunity to improve voltage deviation, reduce power loss, boost efficiency, and ultimately raise system stability. This can be accomplished by reconfiguring the network and allocating distributed generations (DG) and distribution FACT devices, like distribution static compensator (DSTACOM), in the most effective way while considering the stochastic nature of solar irradiance variations, uncertainties, and load variations. The presented article enumerates the planning for optimal photovoltaic distributed generation (PVDG) and DSTATCOM device with Network Reconfiguration (NRX) using a hybrid marine predator jellyfish algorithm (HMPJA). Inspired by the coordinated movements of jellyfish and the effective hunting techniques of marine predators such as sharks, the HMPJA was created. It seeks to improve the exploration, exploitation, resilience, and flexibility of optimization algorithms in handling challenging situations by combining these tactics. Inspired by the social behavior of jellyfish and marine predators, this hybrid algorithm is used to evaluate the techno-economic benefits of installing PVDG and DSTACOM in radial PDN with reconfiguration. With multi-objective function Cost reduction, voltage stability enhancement, and voltage profile (VP) augmentation in radial PDN are the primary goals of the current study. The IEEE 33- and 69-bus systems are used to demonstrate the efficacy of the HMPJA, demonstrating notable decreases in energy and power losses and improved VP with overall net profit. A comparison of the suggested strategy with other nature-inspired alternatives demonstrates its superiority. The findings of the proposed approach provide valuable insights for distribution system planning and operation in future grids with high renewable energy source penetration.*

Key words: *Marine Predator Algorithm, Jellyfish Search, Radial Distribution System, DSTATCOM, PVDG, Reconfiguration*

Received November 25, 2024; revised January 18, 2025; accepted February 03, 2025
Corresponding author: Pragya Guru
The NorthCap University, Gurugram, India
E-mail: pragyaguru18@gmail.com

1. INTRODUCTION

As we are transitioning toward sustainable energy technologies, it is necessary to develop innovative strategies for effective PDN planning, particularly photovoltaic systems, which present opportunities and challenges. This study investigates a probabilistic approach to optimal PDN planning that incorporates integrated photovoltaic-based distributed generation (PVDG) and Distribution Static Synchronous Compensators (DSTATCOM). To optimize system performance under fluctuating conditions, exploring network reconfiguration (NRX) strategies is crucial. This research aims to counteract uncertainties caused by solar irradiation and demand changes by optimizing the reliability and efficiency of PDN minimizing operational costs and optimizing the incorporation of sustainable energy sources through advanced probabilistic modeling. The findings will provide valuable insight into the construction of resilient PDNS that can adapt to the dynamic energy landscape and aid sustainable development initiatives. This research is intended to guarantee a more reliable and environmentally friendly energy future.

1.1. Motivation

The two main components of the electrical system are the transmission and distribution networks [1]. Planning an efficient PDN is complicated by the fact that solar irradiance is unpredictable, which adds a significant amount of uncertainty to power generation. As we are transitioning to more sustainable energy models, there is a need to deploy DG sources, particularly solar PVDG. By using PVDG countries can reduce their carbon emission and become energy-independent as they work to meet renewable energy targets.

To further improve power quality and voltage stability in these developing networks, DSTATCOM can be implemented. PV systems and DSTATCOM work together to maximize operating efficiency. However, this synergy makes planning more difficult and calls for creative solutions that consider dynamic variations in supply and demand.

By altering the network topology, operators can increase load distribution, boost dependability, and lower losses. Reconfiguration is a potent methodology for managing the uncertainties and results brought on by renewable energy sources as it enables real-time reactions to variations in generation and demand. However, incorporating NRX into a probabilistic planning paradigm necessitates a sophisticated comprehension of how PV-based DG, DSTATCOM, and fluctuating load conditions interact.

By optimal allocation of PVDG and DSTACOM in a reconfigured distribution system enhances the reliability of the grid by mitigating voltage fluctuations, and also increasing economic efficiency by reducing power losses.

1.2. Literature Review

Sectionalizing lines are closed, as opposed to open tie lines which are open under normal conditions. [2]. By rearranging the sectionalizing and tie lines, the bus system can be reconfigured to its ideal state [3]. Reconfiguration aims to alleviate overload in the PDN, boost stability and dependability, decrease losses, and enhance voltage profile (VP).

In [4] authors Merlin and Back found the idea of reconfiguring a PDNS. there are some old studies show the importance of the reconfigured network. In [5], a self-adaptive modified optimization algorithm was used to suggest the reconfiguration problem in terms of dependability. [6] presents a multi-step resolution process in which Harris Hawks algorithm is essential to achieving the intended outcomes. In [7], NRX in existing networks was approached using a modified Selective Particle Swarm Optimization (PSO) while considering various loading situations. In [8], Multi-Objective Random-Key Genetic was introduced to enhance energy loss in electric PDNS by allocating meters.

Traditional PDNSs have changed because of the integration of DG, particularly from renewable energy sources (RER) like solar and wind. PVDG is chosen over other RERs for numerous reasons, including There are no moving parts, exceptional reliability with a 25-year warranty, and a less visible design compared to wind turbines, space-saving and wind-resistant, as panels can be put on a roof, Environmental, economic, and electricity network performance are closely linked for this type.

Several efforts have been made to integrate PVDG into the electricity supply. The authors of [9] used the Bat algorithm to optimize the integration of capacitors and distributed generation while accounting for load variations. Ref [10] uses PSO to create a voltage stability index for the ideal DG allocation. In [11], a chaotic symbiotic organism search method was created to deploy DG units in a radial system, resulting in improved VP and reduced power loss. In article [12], an improved gravitational search method was used to examine NRX using DGs. The goal was to increase transient stability, reduce loss, and lower operating costs in the PDNS. A hybrid algorithm is used in [13] to insert multiple DG units for the desired outputs. The GWO method for choosing the best for line parameter calculation by the authors is reference [14]. The optimal PVDG size and location is determined using PSO and weighted-sum method in [15]. Authors in [16] find the optimal position for PV by using voltage collapse proximity index.

From a technological and financial standpoint, the best distribution of distributed generators using shunt compensators is an efficient approach. DFACTS are widely incorporated. Manuscript presented in [17] shows deployment of DFACT devices with DG in PDNS. DSTACOM is a voltage source converter, shunted to a specific bus DSTATCOM is a productive device that operates as a voltage source converter that is shunted to a specific bus and able to reduce system harmonic, balance the load, and significantly improve the system's efficiency. Additionally, by injecting a regulated voltage, it responds quickly to either absorb or inject reactive power. Furthermore, it has no operating problems such as resonance or transient harmonics, in contrast to series or shunt capacitors [18, 19, 20]. In [21] authors represent hybrid plant growth simulation PGS-PSO algorithms for NRX in the presence of the multiple DG units.

The immune algorithm was used in [22] to determine the DSTATCOM's location and dimensions to minimize losses. The Harmony Search Algorithm was used in [23] to optimize the DSTATCOM location and dimensions for loss minimization. In [24], Using the Differential Evolution (DE) technique, the DSTATCOM's location and size were adjusted with the optimal network design to minimize losses. The location and dimensions of the DSTATCOM for improvement have been determined using the binary gravitational search approach [25]. Combining the operators of several metaheuristic algorithms is one sort of hybridization that performs better in several areas, such as convergence speed and solution quality [26, 27]. To find the capacity and best location for the DSTATCOM for a multi-objective function with load demand uncertainties, the authors in [28] used the imperialist competitive approach.

An ant colony method and a fuzzy approach are used in [29] to determine the best distribu tion of PVDG and DSTATCOM. To reduce expenses, losses, and the VP, the DSTATCOM and DG have been assigned using the Bacterial Foraging optimization approach [30]. To sustain the voltage and minimize losses, the PSO has been used to distribute the DG and DSTATCOM [31]. The authors in [32] optimized the locations and dimensions of the DSTATCOM and DG using the whale optimization (WOA) method to cut expenses and losses. In [33] authors work compares WOA, DE, GWO and their quasi-opposition-based variants for reactive power planning with FACTS devices. To reduce loss and improve VP and stability, the lightning search technique is used in [34] for DG-DSTATCOM allocation.

To minimize voltage variations, cost, and loss, the DSTATCOM and DG allocation has been optimized using a hybrid lightning search algorithm and the simplex approach [35]. In [36], the best PVDG, DSTATCOM, and energy storage units have been chosen to minimize costs, enhance voltage performance, and increase dependability. The Harris Hawks technique was used by the authors in [37] to determine the ideal locations and sizes at various power factor values. To achieve a resilient and effective PDNS, the synergy between the integration of the PVDG-DSTATCOM and the optimal reconfiguration plays a vital role.

Numerous studies emphasize the benefits of employing probabilistic models as opposed to deterministic ones. Authors in [38] load uncertainties are considered to see the impact while placing renewable DG in the system. Results in [39] shows, the proposed MALO-based optimization framework effectively addresses the challenges of PV-DG and DSTATCOM integration in distribution systems with uncertainties, leading to a more reliable and efficient grid operation. This literature review concludes the importance of PDNS planning in the presence of PVDG and DSTATCOM under probabilistic modeling and enhances the system performance by network resilience.

1.3. Research Contribution

It has been determined from previously published research that there has never been an investigation into network reconfiguration with the solar PVDG and DSTATCOM integrated into the PDN using hybridized marine predator and jellyfish search algorithms. This study adds to the published literature by utilizing the hybrid marine predator and jellyfish search technique. This hybrid approach leads to a faster convergence rate to using either individual algorithms, or enhanced exploration and exploitation processes. Hybrid algorithm has increased robustness and versatility and enhanced solution quality. This article presents the solution to the optimal power planning problem integrating PVDG and DSTATCOM, in a reconfigured network considering the uncertainties associated with four seasonal variations in solar irradiance and the load for summer, winter, spring, and autumn. The method is implemented on the widely used IEEE 33-bus standard. To determine the efficacy of the suggested technique, two case studies combining solar PVDG with and without uncertainties are studied, and the outcomes of the test are further compared to previously published results. The following is a summary of the contributions made to the article.

a) Finding the optimal installation of PVDG sources and DSTATCOM, and reconfiguring the distribution network to account for the impact of load demand and solar irradiance uncertainty.
b) A multi-objective optimization problem is formulated that involves minimizing cost, power losses and voltage deviation and improving the Voltage Stability Index using hybridisation of two nature-inspired algorithms.
c) The load and the generation have been considered as random variables. Using historical data spanning three years, the uncertainty of the solar radiation and load

demand is modelled as gaussian distribution model and beta distribution model, respectively.

d) Based on the simulation results, this research methodology for constructing large-scale PDN at all load levels is far more practical and efficient.

2. MODELLING

2.1. Line Modelling

Fig. 2 displays a simplified schematic of Fig. 1. At the u^{th} bus, the injected complicated power is provided as,

$$s_u = p_u + jq_u \tag{1}$$

Where, q_u and p_u is real and reactive power load at the u^{th} bus, respectively.
Eq. 2 represents current injected at the u^{th} bus (i_u),

$$i_u = \frac{p_u - jq_u}{v_u^*} \tag{2}$$

Where the voltage at u^{th} bus is denoted by v_u.
Eq. (3) gives the real power loss in a branch connecting nodes u and $u+1$.

$$p_{loss}(u,u+1) = i_u^{\,2} \cdot r \tag{3}$$

$$p_{loss}(u,u+1) = \left(\frac{p_u - jq_u}{v_u^*}\right)^2 \cdot r \tag{4}$$

$$p_{loss}(u,u+1) = \left(\frac{p_u^{\,2} + q_u^{\,2}}{v_u^{\,2}}\right) \cdot r \tag{5}$$

2.2. Integrated Photovoltaic-Based Distributed Generation

Positioning the PV unit at an ideal site and size facilitates reducing real power losses, enhancing VPs, minimizing environmental consequences, improving overall energy system performance, and alleviating PDN overload. Due to the random nature of solar PV-based plants, the network experiences an increase in uncertainty. As a result, precisely calculating PV power is difficult. Solar radiation intensity, absorption capacity, panel surface, and cell temperature all affect how much power PV systems can produce. Because solar radiation is stochastic, the related output power fluctuates. The PV output power (P_{rPV}) is given by

$$P_{rPV} = \begin{cases} P_{rated}\left(\dfrac{G_S^{\,2}}{G_{stdn} \times G_C}\right) & for\ 0 < G_S < G_C \\ P_{rated}\left(\dfrac{G_S}{G_{stdn}}\right) & for\ 0 < G_S < G_C \\ P_{rated} & for\ G_{stdn} \le G_S \end{cases} \tag{6}$$

where the standard solar irradiance G_{stdn}, is 1000 W/m^2 is and G_S shows solar irradiance W/m^2. G_C stands for a specific point of irradiance.

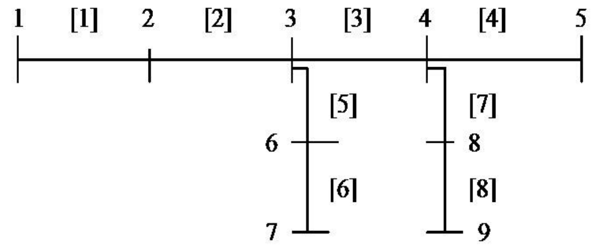

Fig. 1 Illustrative PDNS

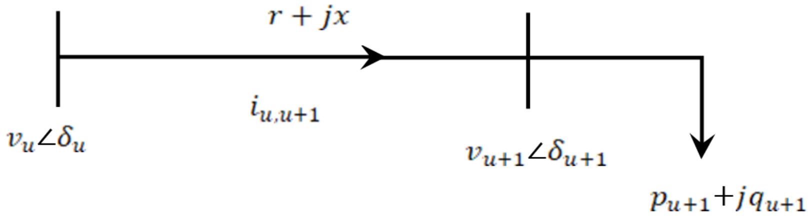

Fig. 2 One-line diagram

2.3. DSTATCOM Modeling

DSTATCOM modeling typically involves a voltage source converter, energy storage system, and control algorithms. DSTATCOM modeling incorporates simulating the behavior of the power electronic devices for reactive power management in electrical systems to enhance power quality, improve voltage stability, and reduce losses. Under various operating situations, DSTACOM modeling helps to ensure reliable grid operation by analyzing system dynamics and optimal integration of renewable energy sources. This technique facilitates the evaluation of performance metrics, such as response time and efficiency, which leads to effective design and deployment in contemporary power systems. DSTATCOM reactive power is expressed as follows, with real power set to zero:

$$q^{DSTATCOM} = \left(\frac{v_u^2}{x_u}\right) - \left(\frac{v_u v_{u+1}}{x_u}\right)\cos\delta \tag{7}$$

2.4. Network Reconfiguration

The act of changing the structure of PDN to optimize the system performance by adjusting the switching arrangement of the nodes and branches is known as network reconfiguration. Wisely opening or closing switches during varying load conditions or during maintenance to minimize losses, redistribute power flows and to ensure uninterrupted service is an essential part of smart grid technologies as they develop and try to regulate sophisticated distribution networks. The feeder power loss following the reconfiguration is given by

$$p'_{loss}(u,u+1)=\left(\frac{p_u'^2+q_u'^2}{v_u'^2}\right)r \tag{8}$$

The net power losses of the new structure can be obtained by,

$$\Delta p^r_{Tloss}=p'_{Tloss}-p_{Tloss} \tag{9}$$

2.5. Probabilistic Modeling

Probabilistic modeling in the PDN planning plays an important role for enhancing resilience and improved resource placement. This strategy is important in light of changing energy scenarios and the merging of dispersed energy resources, specifically with regard to load demand and solar irradiation. The load demand and PV unit have been modelled probabilistically using the location historical data. Three years' worth of hourly statistics on solar irradiation and load demand were taken into account in this study. Consequently, the year is divided into four different seasons. A day (24 hours) within a season is used to characterize the stochastic behaviour of the PV and load demand within that season. Every year, there are 96 time periods (four seasons, twenty-four hours). By applying the data regarding the same hours of the day, the probability density function (pdf) for each season is determined. Thus, the 270 solar irradiances and load demand for each period—three years, three months per season, and thirty days per month—are used to generate the necessary hourly PDFs. The following is a description of the PV system and probabilistic load demand model.

2.2.1. Solar irradiance modeling

Using the data on solar irradiance, a beta pdf $f_B(g_{sr})$ has been generated for each hour, which can be explained as follows [40] [41]:

$$f_B(g_{sr})=\begin{cases}\dfrac{\Gamma(\alpha_{sr}+\beta_{sr})}{\Gamma(\alpha_{sr}),\Gamma(\beta_{sr})}g_{sr}^{(\alpha_{sr}-1)}\cdot(1-g_{sr})^{(\beta_{sr}-1)}, & 0\le g_{sr}\le 1:\alpha_{sr},\beta_{sr}\ge 0\\ 0, & otherwise\end{cases} \tag{10}$$

where Γ is gamma function and α_{sr}, β_{sr} are the beta parameters for each period.

Using the historical data, these parameters can be established as follows [42], [43]:

$$\beta_{sr}=(i-\mu_{sr})\times\left(\frac{\mu_{sr}\times(1+\mu_{sr})}{\sigma_{sr}^2}-1\right) \tag{11}$$

$$\alpha_{sr}=\frac{\mu_{sr}\times\beta_{sr}}{1-\mu_{sr}} \tag{12}$$

where μ_{sr} and σ_{sr} are each period's solar irradiance mean and standard deviation.

The continuous beta pdfs are separated into many segments, each of which yields a mean value. A segment's probability of happening at a specific hour can be determined by:

$$prob_t^{g_{sr}} = \int_{g_{sr,t}}^{g_{sr,t+1}} f_B(g_{sr}) dg_{sr,t} \tag{13}$$

where $g_{sr,t}$ and $g_{sr,t+1}$ stands for beginning and ending points of the interval, respectively for interval t. The likelihood that interval t will occur is denoted by $prob_t^{gsr}$. The generated beta pdf of the solar irradiance for a given period can be used to calculate the output power PV for the states of that period (6).

2.2.2. Modelling of Load Dynamics

At each bus, the load demand is modelled using gaussian pdf because it is stochastic. The gaussian pdf of the load demand $f_{nl}(l)$ is specified in eq. (14) [41]:

$$f_{nl}(l) = \frac{1}{\sigma_{ld}\sqrt{2\pi}} \times \exp\left[-\left(\frac{l-\mu_{ld}}{2\sigma_{ld}^2}\right)\right] \tag{14}$$

where the mean and standard deviation of the load demand are given by μ_{ld} and σ_{ld} for each period. The following is an expression for the segment's occurrence probability at a given hour:

$$prob_t^l = \int_{l_t}^{l_{t+1}} f_{nl}(l) dl \tag{15}$$

where the beginning and ending points of the interval t are denoted by l_t and l_{t+1} respectively. $prob_t^l$ symbolises the probability that interval t will occur.

2.6. Integrated Model of Solar Irradiance and Probabilistic Load

The probabilistic solar irradiance and load model are presented in the preceding sections. An integrated probability model of the PV load is generated using these. Convoluting the probability of solar irradiance and load demand allows one to compute the integrated model of the interval t in the manner described below:

$$P_{int,t} = prob_t^{gr} \times prob_t^l \tag{16}$$

The objective function specified in (17) should be computed for each state and proportionate to the combined probability model in terms of weight, representing the state's probability of occurrence over the planning period. An hour is represented by each time section. This indicates that each variable has several values for every period. However, we have simply displayed the variables' mean or expected values for simplicity's sake.

3. PROBLEM FORMULATION

Promoting the technical and fiscal benefits of effective planning for the integration of PVDG and DSTATCOM in the power system is the primary task this work presents. Although load demand and solar irradiation is difficult to predict accurately, it should be mentioned that the planning period is three years long, with 91.25 days in each of the four seasons. The multi-objective function in (17) tends to minimize voltage deviation, cost, and VSI.

3.1. Objective Function

$$\min\ f = \min(\omega_1 \times Obje_1) + \min(\omega_2 \times Obje_2) + \min(\omega_3 \times Obje_3) \tag{17}$$

where $Obje_1$, $Obje_2$ and $Obje_3$ represents voltage deviation, cost and VSI. The weighting factors ω_1, ω_2 and ω_3 are governed by (18).

$$|\omega_1| + |\omega_2| + |\omega_3| = 1 \tag{18}$$

and

$$Obje_1 = \frac{TVDev_W}{TVDev_{Wo}}$$

$$Obje_2 = \frac{cost_W}{cost_{WO}}$$

$$Obje_3 = \frac{1}{\sum_{n=1}^{N_b} VSID_n}$$

where $TVDev_{Wo}$ and $cost_{WO}$ shows the total voltage deviation and total cost without insertion of the PVDG or DSTATCOM and $TVDev_W$ and $cost_W$ shows the total voltage deviation and total cost with the insertion of the PVDG or DSTATCOM

Enhancing the VP by reducing the voltage deviations is stated in (19)

$$TVDev = 91.25 \times \sum_{e=1}^{N_s} \sum_{f=1}^{24} \sum_{g=1}^{NB} (V_n - 1) \tag{19}$$

The total annual cost $cost_W$ can be formulated as follows:

$$cost_W = cost_{loss} + cost_{grid} + cost_{PV} + cost_{Recon} + cost_{ST} \tag{20}$$

where $cost_{loss}$, $cost_{grid}$, $cost_{PV}$, $cost_{Recon}$ and $cost_{ST}$ represents the cost of power loss, energy loss, PV unit and DSTATCOM installation cost and cost of NRX, respectively.

$$cost_{loss} = c_{loss} \times 91.25 \times \sum_{e=1}^{N_S} \sum_{f=1}^{24} \sum_{g=1}^{NB} p_{loss(e,f,g)} \tag{21}$$

Where c_{loss} represents the cost of the energy loss. N_S represents the number of seasons per year and is equal to 4. NB represents the number of network branches.

The cost of power injection at the substation is given in (22):

$$cost_{grid} = c_{grid} \times 91.25 \times \sum_{e=1}^{N_S} \sum_{f=1}^{24} p_{loss(e,f)} \tag{22}$$

The cost of DSTATCOM installation is given in (23):

$$cost_{ST} = C_{ST} \times Q_{ST} \times \frac{(1+\alpha)^{N_S} \times \alpha}{(1+\alpha)^{N_S} - 1} \tag{23}$$

where DSTATCOM's rated kVAr, Capital cost is represented by Q_{ST}; and C_{ST}; α denotes the asset rate of return DSTATCOM N_s is the lifetime of the DSTATCOM in years;. The cost of the PV system consists of fixed and variable cost given by (25) and (26).

$$cost_{PV} = cost_{fixed} + cost_{Vari} \tag{24}$$

$$cost_{fixed} = CRF \times C_{PV} \times P_{rated} \tag{25}$$

$$CRF = C_{Op\&Mt} \times \sum_{e=1}^{N_S} \sum_{f=1}^{24} p_{PV(e,f)} \tag{26}$$

where the operation and maintenance cost is denoted by $C_{Op\&Mt}$,; P_{PV} stands for output power of the PV unit given in eq. (6).

Enhancing stability by improving the voltage stability index as given in (27):

$$VSID = 91.25 \times \sum_{e=1}^{N_S} \sum_{f=1}^{24} \sum_{g=1}^{NB} VSID_g \tag{27}$$

where

$$VSID_g = \left|V_g\right|^4 - 4(P_{mn} X_n - Q_{g+1} R_n)^2 - 4(P_{n+1} X_n + Q_{g+1} R_n)\left|V_g\right|^2 \tag{28}$$

2.1. Constraints

The equality and inequality constraints are specified below.

$$P_{slack} + \sum_{g=1}^{N_{pv}} P_{pv}, g = \sum_{g=1}^{N_b} p_{loss}, g + \sum_{g=1}^{NB} P_{L,g} \tag{29}$$

$$Q_{slack} + \sum_{g=1}^{N_{pv}} Q_{pv}, g = \sum_{g=1}^{N_b} q_{loss}, g + \sum_{g=1}^{NB} Q_{L,g} \tag{30}$$

$$\text{Maintaining radiality } N_{mainloop} = (N_b - NB) + 1 \tag{31}$$

The other operational constraints are bus voltages within ± 5%, thermal limit for ampacity, real and reactive limits, DG real and reactive power generation. The number of sectionalising switches is given by (32)

$$N_b = NB - 1 \tag{32}$$

N_b is total no. of nodes in the system.

4. SYNERGISTIC MARINE PREDATORS-JELLYFISH SEARCH OPTIMIZATION ALGORITHM

4.1. Marine Predators Algorithm

The ocean predator interactions and Levy and Brownian movement tactics in a marine predator algorithm (MPA) [44] are explained below

4.1.1. Initialization

Using (33), MPA derives randomly its initial solutions in terms of l^{th} prey's position (Pry_l^m)

$$Pry_l^m = lbd^m + rand(0,1) \times (ubd^m - lb^m) \tag{33}$$

where rand is random integer between 0 and 1. The lower and upper bounds on the m^{th} dimension are denoted by lbd^m and ubd^m, respectively.

4.1.2. Optimization

The three stages of the algorithm mimic the methods used by predators to capture their prey. A distinct velocity ratio is considered in each of the MPA three stages. Every phase has a set number of iterations assigned to it.

Phase 1 (Exploration stage): The prey moves more quickly (high velocity) than the predator.

When Itr < 1/3 Maxitr, Phase 1 is chosen. (34) is used to update the solutions.

$$Pry_l = Pry_l + P.RV \times stepsz_l \tag{34}$$

$$stepsz_l = RV_{Bl}\,(Elite - R_{Bl} \times Pry_i) \tag{35}$$

$$RV_{Bl} = \frac{1}{\sqrt{2\pi}}\exp\left(-\frac{x^2}{2}\right) \tag{36}$$

where *stepsz* is step size, coefficient P is equal to 0.5. The matrices RV and RV_{Bl}, both of dimension 1 × dim, are composed of random values within the interval (0,1) and numbers produced by the Brownian movement, respectively. Elite is currently the best available option.

Phase 2 (Exploration and Exploitation stage): Unit velocity ratios show that the predator and prey move almost simultaneously. There is an equal distribution of solutions between exploration and exploitation. Exploration is managed by the Predator, and the victim is being taken advantage of. The Levy function and Brownian motion, respectively, control the movement of the predator and the prey. Updated for the one-half of the population are the following formulae.

$$stepsz_l = RV_{Ll}\,(Elite - RV_{Ll} \times Pry_l) \tag{37}$$

Given random walk data generated by the Levy function, RV_{Ll} is a matrix of dimension equal to that of RV.

$$L(Pry_{jl}) \approx |\omega|^{1-a} \tag{38}$$

where a is in the range (1, 2) that determines the scale, which is taken to be 1.5, and ω is the flight length.

The following integral shows the Levy function's probability distribution:

$$f_L(\omega; a, \gamma) \approx \frac{1}{\pi}\int_0^{\infty} \exp(-\gamma q^a)\cos(q\omega)dq \tag{39}$$

$$f_L(\omega; a, \gamma) \approx \frac{\gamma\Gamma(1+a)\sin\left(\frac{\pi a}{2}\right)}{\pi\omega^{(1+a)}}\ \omega \to \infty \tag{40}$$

where Γ represents Gamma function.

The population is regulated using (41-43) for exploration.

$$Pry_j = Pry_j + P.CVF \times stepsize_j \tag{41}$$

$$stepsz_l = RV_{Bl}\left(Elite \times RV_{Bl} - Pry_{jl}\right) \tag{42}$$

$$CVF = \left(1 - \frac{ITR}{Max_{Itr}}\right)^{\left(2 \times \frac{ITR}{Max_{Itr}}\right)} \tag{43}$$

where the step size is governed by CVF.

Input: No. of predators (N_{pred}), maximum iteration (Max_{it}), FADGs, problem's specifications, and parameters
Output: *Elite*
% Initialization
Create initial predators within the problem space randomly by equation 33
Calculate Predators' fitness and select Elite

for *It* = *1*: Max_{it}
    % Optimization
    if $It < \frac{1}{3}\ Max_{it}$
        Update Predators by equation 34
    else if $It > \frac{1}{3}\ Max_{it}$ && $It < \frac{2}{3}\ Max_{it}$
        Update first half of the Predators by equation 36
        Update second half of the Predators by equation 41
    else if $It > \frac{2}{3}\ Max_{it}$
        Update Predators by equation 44
    end if
    Calculate Predators' fitness and update Elite

    % Marine memory
    Apply greedy selection mechanism

    % Eddy formation
    Update Predators by equation considering the FADGs
    Calculate Predators' fitness and update Elite

    % Marine memory
    Apply greedy selection mechanism
end for
Return *Elite*

Fig. 3 Pseudocode for MPA

Phase 3 (Exploitation stage): The predator has higher velocity than the prey, making it faster. Predators are kept up to date during this phase. Eq. (44-45) provided a mathematical formulation of this phenomenon.

$$Pry_l = Elite + P.CVF \times stepsz_l \tag{44}$$

$$stepsz_l = RV_{Ll}(Elite \times RV_{Ll} - Pry_l) \tag{45}$$

4.1.3. Eddy formation

This stage is similar to Fish Aggregating Devices (FAGD) which causes predators to alter their behaviour. The FAGD is expressed mathematically as below:

$$Pry_l = \begin{cases} Pry_l + CF \times \left[lbd + RV \times (ubd - lbd)\right] \times U & r \le FAGDs \\ Pry_l + \left[FAGDs \times (1-r) + r\right](X_{r1} - X_{r2}) & otherwise \end{cases} \tag{46}$$

$$U = rand(1, dim) < FAGDs \tag{47}$$

where X_{r1} and X_{r2} are two randomly chosen solutions from the population, U is a binary vector and the *FAGDs* is 0.2.

4.1.4. Predator memory

After a successful feeding expedition, marine predators return to areas they have a good recollection of [35]. This capacity is replicated by keeping memories in MPA. To ascertain which answer is superior, the solutions from each iteration are compared to the prior one. Fig. 3 displays the pseudocode.

4.2. Artificial Jellyfish Search Algorithm

4.2.1. Initialization

To replicate the movement of jellyfish in a swarm or while traveling towards the ocean current in quest of food, an artificial JFSA [45] was created. The colony of jellyfish is started at random. As a result of low population variety, there may be a risk of trapped local optima and sluggish convergence. The logistic chaotic map, as presented in Equation (54) provides a lower likelihood of early convergence and a wider range of initial populations compared to random initialization.

$$JSA_{i+1} = \eta JSA_i(1 - JSA_i), 0 \le JSA_0 \le 1 \tag{48}$$

where JSA_i is the logistic chaotic value; JSA_0 is varied to generate the initial jellyfish population, $JSA_0 \notin \{0, .25, .5, .75, 1\}$, and 4 is the value for the parameter η.

4.2.2. Ocean current

The mean of every jellyfish's vector to the one currently occupying the optimal position represents the movement of the ocean current and is represented as (49).

$$\overrightarrow{Direction} = \frac{1}{N_{JFP}} \sum (JS^* - e_c JSA_i) \tag{49}$$

where N_{JFP} represents number of jellyfishes in swarm and JSA^* represents the best jellyfish while attraction govern factor is represented by e_c.

$$\overrightarrow{Direction} = JSA^* - e_c \frac{\sum JSA_i}{N_{JFP}} = JSA^* - e_c \mu_{JSA} \tag{50}$$

where μ_{JSA} shows the mean position of all the jellyfishes in an ocean

$$e_c = \beta_{JSA} \times rand\left(0,1\right) \tag{51}$$

where β_{JSA} is distribution coefficient whose value is taken as 3.

The new jellyfish position is defined as:

$$JSA_i(t+1) = JSA_i(t) + rand(0,1) \times \overrightarrow{Direction} \tag{52}$$

$$JSA_i(t+1) = JSA_i(t) + rand(0,1)\left[JSA^* - (\beta_{JSA} \times \mu_{JSA} \times rand(0,1)) \right] \tag{53}$$

4.2.3. Jellyfish swarm

The majority of jellyfish exhibit passive motion (type A) at first around their initial sites, as the jellyfish swarm is still forming. They start to move more actively (type B) as time progresses.

$$JS_i(t+1) = JS_i(t) + \gamma_{js} \times rand(0,1) \times (ub - lb) \tag{54}$$

where γ_{js} represents the motion coefficient and its value is taken as 0.1.
The direction of the motion of the jellyfish in search of its food and its updated location in the search space are simulated by (43) and (44), respectively.

$$\overrightarrow{Dir} = \begin{cases} JS_j(t) - JS_i(t) \;\; if \;\; f(JS_i) \geq f(JS_i) \\ JS_i(t) - JS_j(t) \;\; if \;\; f(JS_i) < f(JS_i) \end{cases} \tag{55}$$

where $f(JS_i)$ *and* JS_i represent the objective function and jellyfish location.

$$JS_i(t+1) = JS_i(t) + \overrightarrow{step} \tag{56}$$

where

$$\overrightarrow{step} = rand\left(0,1\right) \times \overrightarrow{Dir} \tag{57}$$

4.2.4. The control mechanism

The type of jellyfish motion and its gradual transition from one swarm to another are determined with the aid of the time control function ($CF(t)$) [0,1]. If the jellyfish value is more than or equal to CF_0, it floats with the ocean current; if it is less than CF_0 it stays with the swarm.

$$CF(t) = \left| \left(1 - \frac{1}{Max_{Itr}}\right) * (2rand(0,1) - 1) \right| \tag{58}$$

where Max_{itr} represents the maximum number of iterations.

4.2.5. Boundary conditions

A jellyfish will eventually return if it leaves the boundaries of the search area. As an illustration of reintegration process,

$$\begin{cases} JSA'_{i,d} = (JSA_{i,d} - U_{b,d}) + L_b(d) & if\ JS_{i,d} > U_{b,d} \\ JSA'_{i,d} = (JSA_{i,d} - L_{b,d}) + U_b(d) & if\ JS_{i,d} < L_{b,d} \end{cases} \tag{59}$$

where the ith jellyfish location in dth dimension is represented by $JSA_{i,d}$ and its upper and lower bounds in food search space is given by $U_{b,d}$ and $L_{b,d}$, respectively. $JSA'_{i,d}$ is the updated position of the ith jellyfish.

In Learning automata (LA), extended learning vector in is provided by the following equation:

$$P_r = \{P_1, P_2, \dots \dots, P_{nm}\} \tag{60}$$

$$P_r = \begin{bmatrix} P_{1JSA1} & \cdots & P_{nmJSA1} \\ \vdots & \ddots & \vdots \\ P_{1JSNoJSA} & \cdots & P_{nmJSNoJSA} \end{bmatrix} \tag{61}$$

With more plausible values, the optimal motions have a higher chance of being selected. Conversely, non-optimal solution movements have smaller probability values and are therefore less likely to be selected.

$$Action\_index = find\left(rand(0,1) \le \frac{p_i}{\sum_{i=1}^{nm} p_i}, 1'\ first' \right) \tag{62}$$

where *find* is a searching function and the probability of i^{th} motion is denoted by p_i. JFSA pseudocode is given in Fig. 4.

4.2. LA-based Hybridization

The suggested hybridization of the LA-based HMPJA will increase the algorithms' reliability and overcome the drawbacks of the individual metaheuristic algorithms, such as insufficient jellyfish movements, scattering of jellyfishes in the search space and MP complexity, slow or premature convergence locking in local optima, and sluggish search. Fig. 5 shows the HMPJA flowchart.

```
Input: No. of jellyfish (Nojs), parameters value, maximum iteration, problem's
specifications
Output: JS*

% Initialization
Initialize jellyfishes using Logistic chaotic map using equation no. 59
Calculate JS's fitness and select JS*

For It = 1: Max_It
        for i = 1: Nojs
                Calculate time control parameter using equation 58
                if C(It) ≥ C_0
                        % Ocean current Movements
                        Update ith jellyfish using equation 52
                else
                        % inside swarm movement
                        if rand(0,1) ≥ 1 − C(It)
                                % Passive Motion
                                Update ith jellyfish using equation 54
                        else
                                % Active motion
                                Update ith jellyfish using equation 56
                        end if
                end if
                Check ith jellyfish feasibility and apply greedy selection mechanism
                Calculate fitness of the ith jellyfish and update JS*
        end for
end for
```

Fig. 4 Pseudocode for JSA

5. SIMULATION RESULTS AND DISCUSSION

The optimal operation is simulated under uncertainty. The one-line diagram of IEEE 33- and 69-bus system are shown in Fig. 6 and Fig.7, respectively. Table 1 displays these systems' initial power flow solutions. The load flow calculations provide the bus voltages and power losses. In terms of losses and (min) voltage, the HMPJA performs better than the others in every case. For both of the situations under discussion, the optimal operation is obtained by using the recommended technique and compared with the results generated by other algorithms. The simulation is carried out on MATLAB, 64-bit operating system and 4GB RAM. The hybrid algorithm's empirical parameters are set at a maximum of 100 iterations and 10 populations.

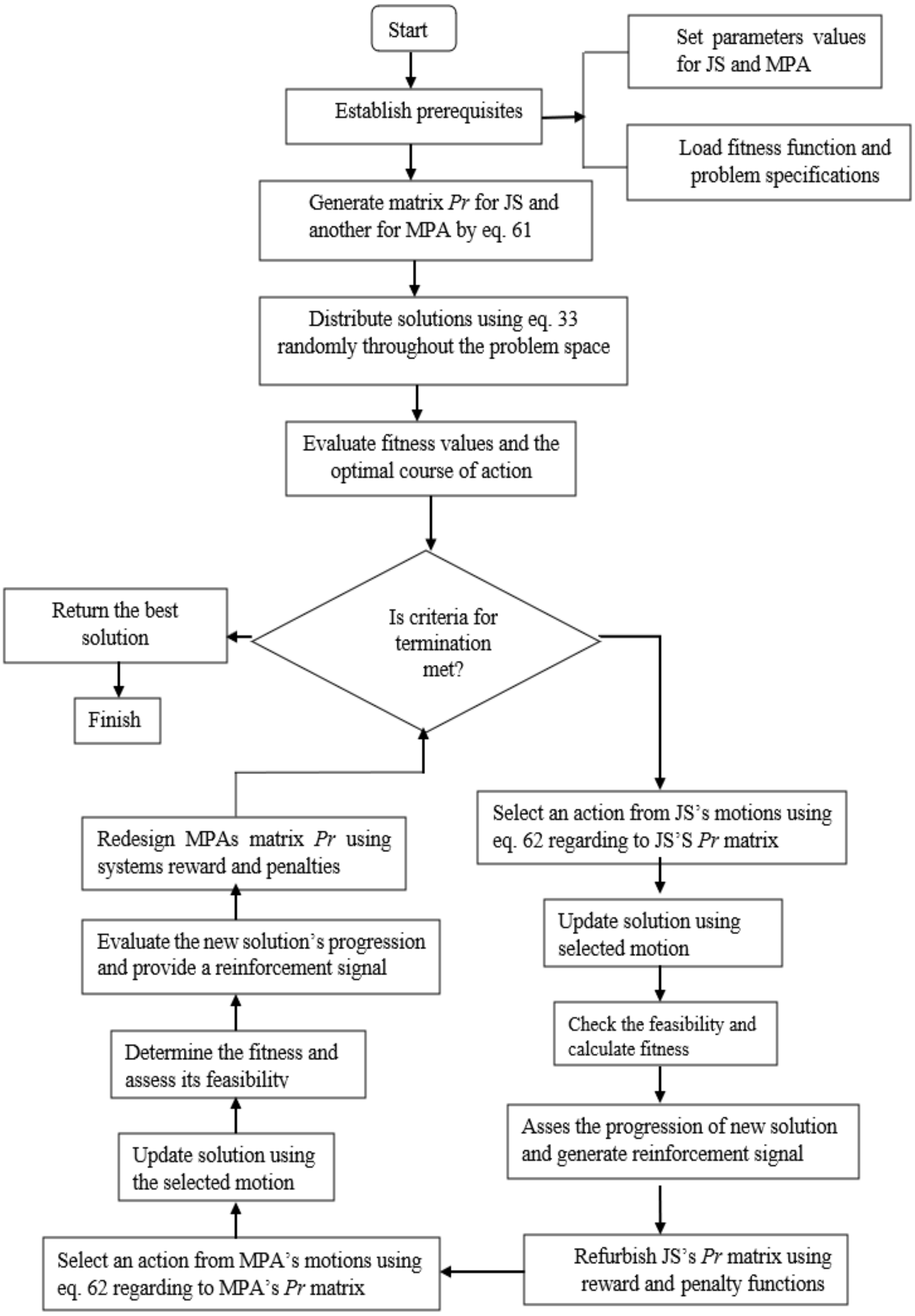

Fig. 5 Flow chart for hybrid HMPJA

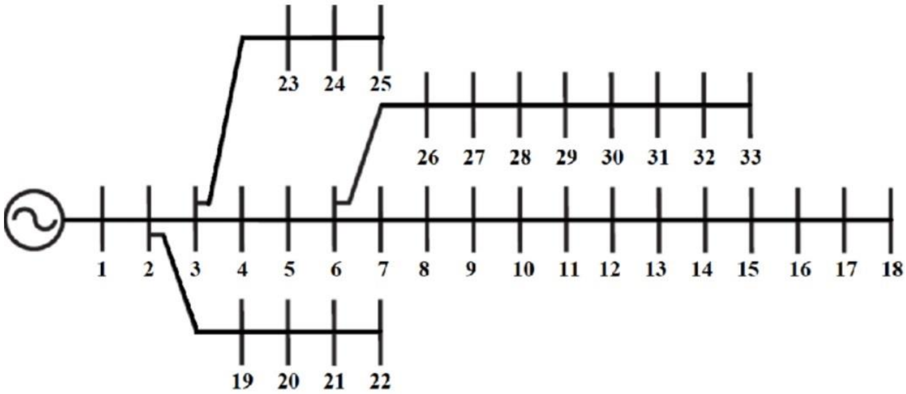

Fig. 6 IEEE 33-bus system

Table 1 The system specification and the base case results of 33-bus system

System Specifications:	33-Bus	69-Bus
NB	33	69
N_{pr}	32	68
V_{sys} (kV)	12.66	12.66
Base MVA	100	100
S_{load} (MVA)	1003.802+j2.694	3.802+j2.694
$P_{Total\ Loss}$ (kW)	202.070	225
$QT_{otal\ Loss}$ (kVAr)	142.437	102.198
V_{min} (pu), bus	0.9131, 18	0.9091, 65

Table 2 The cost coefficients of the PVDG and DSTATCOM

Cost	Parameter	Value
PV	C_{PV}	770 $/kW
	$C_{O\&M}$	0.01 $/kWh
	τ	10%
	NP	20
DSTATCOM	C_S	50 $/kVAr
	α	10%
	ND	30
Grid	C_{loss}	0.06 $/kWh
	C_{grid}	0.96 kWh

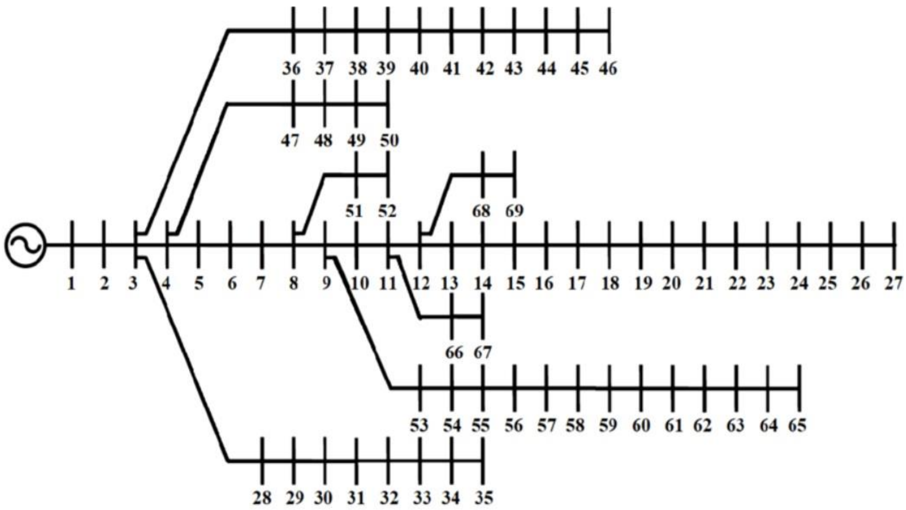

Fig. 7 IEEE 69-bus system

In this instance, the suggested methods are used to solve the optimal planning issue on the considered bus systems while accounting for the uncertainties of the linked load and sun irradiances. Cost reduction, VP, and stability index improvement are among the multi-objective functions for handling the optimum planning issue. It should be noted that this article takes into consideration three years' worth of hourly historical data on load demand and solar irradiation. This has led to the division of each year into four distinct seasons.

A Day (24 hours) within each season is considered to describe the stochastic behavior of the PV and load demand throughout that season. As a result, there are 96 time periods in a year (four seasons of 24 hours). Fig. 8 and 9 show the obtained load profiles and solar irradiance under ambiguous settings.

5.1. IEEE 33-Bus system

The overall cost, TVDEVev, and VSID at the base scenario (without PV or DSTATCOM or NRX included) are 2.438704E+6 $, 1.3427E+4 pu., and 2.29424E+5 pu. respectively. The suggested approach solves the optimal planning issue by including up to two PVDGs and DTSTACOMs, both separately and in an altered network. The PVDG and DSTATCOM cost parameter data are shown in Table 2. The simulation results are shown in Table 3, Table 4 and Table 5 for the optimal integration of PVDG, and DSTATCOM allocation in the reconfigured network and separately by MPA, JFSA and HMPJA for single hybrid and two hybrid system respectively.

When compared to PVDG or DSTATCOM and NRX without insertion, the overall cost is significantly decreased to 1.963071E+6$, or 19.5%, and 2.398893EC6 or (1.632%) respectively when a single hybrid system is included. Additionally, the TVDev is decreased to 1.0150EC4 (24.40%) and 1.2453EC4 (7.25%) respectively for PVDG or DSTACOM placement and NRX.

Table 3 Simulation results for IEEE 33- bus system for single hybrid systems by MPA and JFSA technique

Entity	Base Case	MPA			JFSA		
		PV + DSTATCOM	NRX	PV + DSTATCOM + NRX	PV + DSTATCOM	NRX	PV+ DSTATCOM +NRX
Eloss (MWh)	1.0782	1.0647	1.0050	0.9186	1.0261	1.0257	1.0016
Egrid (MWH)	24.7293	24.4197	23.0504	21.0688	23.5321	23.5252	22.9724
Optimal loc 1	-	2	-	8	13	-	33
Psr1 (kW)	-	1780	-	1527	2007	-	1769
Qds1 (kVAr)	-	100	-	128	100	-	130
TVDev	1.3427 E+4	13312.3768	13545.4377	11638.5159	10912.8123	14902.0637	11584.5484
VSID	2.29424 E+5	229819.4956	229207.9052	237222.5434	241262.1909	225284.2976	239479.5715
Closs ($)	6.4692 E+4	6.3882 E+4	6.0300 E+4	5.5116 E+4	6.1566 E+4	6.1542 E+4	6.0096 E+4
Cgrid ($)	2.374012 E+6	2.344291 E+6	2.212838 E+6	2.067081 E+6	2.259081 E+6	2.258419 E+6	2.205350 E+6
Cpv ($)	0	1.93792 E+5	-	1.66247 E+5	2.18506 E+5	0	1.92594 E+5
Cds ($)	0	530.5	-	679.04	530.5	0	689.65
Ctotal ($)	2.438704 E+6	2.602495 E+6	2.273138 E+6	2.289123 E+6	2.416274 E+6	2.319961 E+6	2.458729 E+6
Tie Switches	33,34,35, 36,37	33,34,35, 36,37	35,36,25, 9, 4	35,36,25, 9, 4	33,34,35, 36,37	28,10,30, 34,5	28,10,30, 34,5

The VSID is increased to 2.41517EC5 (5.27%) and 2.32748EC5 (1.42%) respectively. Aside from that, there is a significant decrease in energy losses and the amount of energy taken from the grid when 13th bus has been designated as the ideal position for the hybrid system for PVDG-DSTACOM allocation, and the PVDG and DSTATCOM have respective sizes of 969kW and 500kVAR. When the allocation is done in the reconfigured network, total cost and voltage deviation are reduced by 24.63% and 29.93% respectively. VSID is improved by 6.78% as compared to base case condition.

Table 4 Simulation results for IEEE 33- bus system for two hybrid systems by MPA & JFSA

Entity	Base Case	MPA			JFSA		
		PV + DSTATCOM	NRX	PV + DSTATCOM + NRX	PV + DSTATCOM	NRX	PV+ DSTATCOM +NRX
Eloss (MWh)	1.0782	0.8454	1.0901	0.9334	1.0041	1.0717	1.0032
Egrid (MWH)	24.7293	19.3909	25.0034	21.4086	23.0318	24.5815	23.0097
Optimal loc 1	-	2	-	11	2	-	2
Optimal loc 2	-	16		3	16		14
Psr1 (kW)	-	500	-	767	100	-	736
Psr2 (kW)	-	500		500	100		100
Qds1 (kVAr)	-	500	-	500	100	-	100
Qds2 (kVAr)	-	500		500	100		100
TVDev	1.3427 E+4	10356.0057	12804.4816	10250.9471	12766.8065	13572.8215	12764.093
VSID	2.29424 E+5	239869.6562	231941.7684	242147.2927	231587.6083	229289.5333	231955.9914
Closs ($)	6.4692 E+4	5.0724 E+4	6.5408 E+4	5.6005 E+4	6.0251 E+4	6.4305 E+4	6.0193 E+4
Cgrid ($)	2.374012E +6	1.861526 E+6	2.400327 E+6	2.055232 E+6	2.211061 E+6	2.359825 E+6	2.208931 E+6
Cpv ($)	0	1.08872 E+5	-	1.37940 E+5	2.1774 E+4	0	9.1016 E+4
Cds ($)	0	5.305 E+3	-	5.305 E+3	1.061 E+3	0	1.061 E+3
Ctotal ($)	2.438704E +6	1.975703 E+6	2.465735 +6	2.198477 +6	2.418957 E+6	2.424130 E+6	2.361201 E+6
Tie Switches	33,34,35,36,37	69,70,71, 72,73	43,69,54, 61,18	43,69,54, 61,18	69,70,71, 72,73	44,17,58, 39,22	44,17,58, 39,22

The output power of the PV unit fluctuates in proportion to changes in solar radiation. In terms of cost, TVDEV, and VSID, Table 5 shows that the results produced by the suggested algorithm. The IEEE 33-bus PDN is also incorporating two hybrid systems. Table 5 shows a significant decrease in the overall cost to 18.71%, and in TVDev is 32.69% in comparison to the basic scenario. VSID is raised by 6.81%. The 11th bus and the 2nd bus are the designated ideal places for the hybrid systems in this instance, and the first PVDG and DSTATCOM have respective sizes of 908 kW and 100kVAR. DSTATCOM and the second PVDG have respective ratings of 100kVAR and 100kW.

Table 5 Simulation results for IEEE 33- bus system for single and two hybrid systems by HMPJA technique

Entity	Base Case	MPA			JFSA		
		PV + DSTATCOM	NRX	PV + DSTATCOM + NRX	PV + DSTATCOM	NRX	PV+ DSTATCOM +NRX
Eloss (MWh)	1.0782	0.82009	1.0606	0.87065	0.9246	0.8541	0.8274
Egrid (MWH)	24.7293	18.8095	24.3256	19.9691	21.2065	19.5894	18.9778
Optimal loc 1	-	13	-	13	8	-	11
Optimal loc 2	-	-	-	-	2	-	2
Psr1 (kW)	-	969	-	1115	1028	-	908
Psr2 (kW)	-	-	-	-	783	-	100
Qds1 (kVAr)	-	500	-	500	100	-	100
Qds2 (kVAr)	-	-	-	-	100	-	100
TVDev	1.3427 E+4	1.0150 E+4	12453.289	9408.1626	11999.1171	9790.8691	9001.2101
VSID	2.29424 E+5	241517.2	232748.3228	244992.9943	234259.0181	242342.869 1	246198.3321
Closs ($)	6.4692 E+4	4.9205 E+4	6.3636 E+4	5.2239 E+4	5.5476 E+4	5.1246 E+4	4.9644 E+4
Cgrid ($)	2.37401 2E+6	1.805718 E+6	2.335257 E+6	1.191703 E+6	2.035830 E+6	1.880587 E+6	1.821868 E+6
Cpv ($)	0	1.05496 E+5	-	1.21392 E+5	2.16764 E+5	-	1.09742 E+5
Cds ($)	0	2.652 E+3	-	2.652 E+3	1.061 E+3	-	1.061 E+3
Ctotal ($)	2.43870 4E+6	1.963071 E+6	2.398893 E+6	1.837986 E+6	2.309131 E+6	1.931833 E+6	1.982315 E+6
Tie Switche s	33,34,3 5,36,37	33,34,35, 36,37	19,36,12, 11,28	19,36,12, 11,28	33,34,35, 36,37	9, 26, 34, 7, 16	9, 26, 34, 7, 16

Fig. 10 shows the system's VP with the DSTATCOM, PVDGs, and NRX in four seasons. It is evident from Fig. 10 that the addition of two-hybrid systems significantly improves the VP compared to the base situation. Based on Table 5, the results of applying the suggested method are superior to those of the published algorithm.

5.2. IEEE 69-Bus system

The proposed approach is also applied to IEEE 69-bus system for optimal planning is PDN under uncertainties. Fig. 8 and Fig. 9 also show the system load profile and solar irradiance under uncertain conditions. By combining single and two-hybrid systems with reconfiguration, the best possible solution to the power planning problem is evaluated.

The results for the 69-bus system are listed in Table 6, Table 7 and Table 8 for single and two hybrid system by using MPA, JFSA and HMPJA respectively. The total cost and TVDev are reduced by 17.69% and 26.00% respectively for a single hybrid system. The VP is shown in Fig. 11. It is seen from the Fig. 11, that the VP is enhanced with PVDG-DSTACOM inclusion in a reconfigured network. For a two-hybrid system, the TVDev is reduced by 43.80%, along with a 21.72% reduction in total cost. The voltage stability is enhanced by 1.57% and 3.39% in single and two hybrid systems respectively. Table 9 shows the superiority of the proposed algorithm while comparing with the previously published articles.

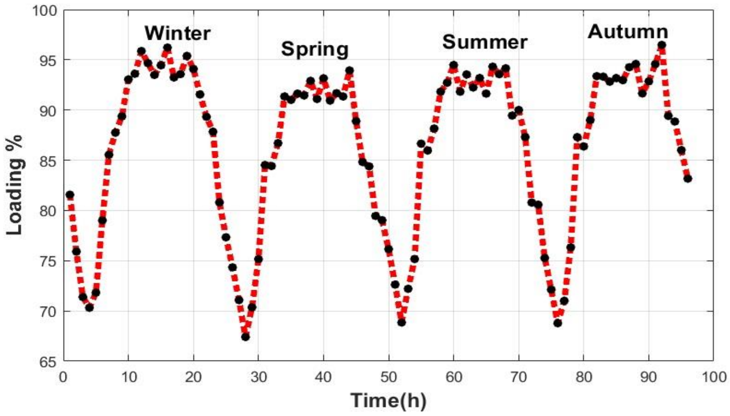

Fig. 8 The hourly load profile across seasons

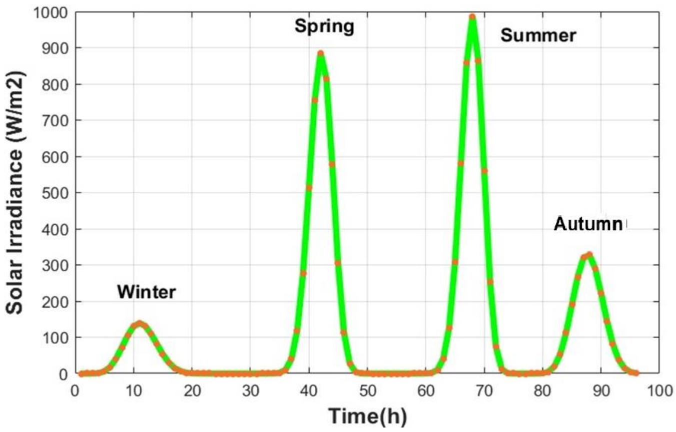

Fig. 9 The variations in solar irradiance throughout the seasons

The following conclusions are derived by the simulation results.

a) A strong and effective tool for PVDG and DSTATCOM optimal planning in the redesigned PDN is made possible by the suggested HMPJA, which outperforms the most recent algorithms.

b) One PVDG and DSTATCOM integrated into the 33-bus system can reduce annual total costs and voltage variations by 24.63% and 28.98%, respectively. The base case voltage stability is improved by 6.35%. The total annual cost can also be reduced by optimally integrating two hybrid PVDG and DSTATCOM in the reconfigured network, with voltage deviations by 18.71 % and 32.96 %, respectively. The improvement in voltage stability over the base case is 6.81%.

c) One PVDG and DSTATCOM hybrid with appropriate integration can reduce the predicted cost and voltage variations in the 69-bus system by 17.67% and 26.00%, respectively. The voltage stability is increased by 1.57% when two hybrid PVDG and DSTATCOM are implemented properly, reducing the overall annual cost and voltage deviation by 21.72% and 43.80%, respectively, and 3.39% when compared to the base scenario with one and two hybrid system respectively.

To solve the challenges of optimal power planning involving the optimal integration of PVDG and DSTATCOM, future study will consider a variety of energy storage solutions, including fuel cells, batteries, hydro-pumps, compressed air, and superconducting magnetic energy storage, electrical vehicle charging stations. The effective implementation of the recommended HMPJA algorithm in the specified technical use gives an assurance to approve the coordinated functioning of FACTS controllers and expand to large-scale interconnected power networks in the future.

Table 6 Simulation results for IEEE 69- bus system for single hybrid systems by MPA & JFSA

Entity	Base Case	MPA			JFSA		
		PV + DSTATCOM	NRX	PV + DSTATCOM + NRX	PV + DSTATCOM	NRX	PV+ DSTATCOM +NRX
Eloss (MWh)	1.19726	1.1513	0.6680	0.5421	1.0796	0.8302	0.7036
Egrid (MWH)	27.44682	26.4059	15.3211	12.4355	24.7614	19.0412	16.1393
Optimal loc 1	-	13	-	17	19	-	12
Psr1 (kW)	-	573	-	695	500	-	666
Qds1 (kVAr)	-	500	-	500	500	-	500
TVDev	1.24867 E+4	10852.5384	11314.4386	8278.4685	12038.1415	17790.0922	14502.1812
VSID	5.40257 E+5	559748.8951	539816.1713	552283.9652	5.49450 E+5	516467 E+5	529179 E+5
Closs ($)	7.1836199 E+4	6.9078 E+4	4.0080 E+4	3.2526 E+4	6.4776 E+4	4.4934 +4	4.3452 +4
Cgrid ($)	2.634895E+6	2.534966 E+6	1.470825 E+6	1.193808 E+6	2.377094 E+6	1.827955 E+6	1.594560 E+6
Cpv ($)	-	6.2383 E+4	-	7.5660 E+4	5.44380 +5	0	7.25087 +5
Cds ($)	-	2.652 E+3	-	2.652 E+3	2.652 E+3	0	2.652 E+3
Ctotal ($)	2.706731E+6	2.669079 E+6	1.510905 E+6	1.348458 E+6	2.988902 E+6	1.872889 E+6	2.365751 E+6
Tie Switches	69,70,71,72,73	69,70,71, 72,73	8,17,11, 53,21	8,17,11, 53,21	69,70,71, 72,73	4,63,19, 69,10	4,63,19, 69,10

Table 7 Simulation results for IEEE 69- bus system for two hybrid systems by MPA & JFSA

Entity	Base Case	MPA			JFSA		
		PV + DSTATCOM	NRX	PV + DSTATCOM + NRX	PV + DSTATCOM	NRX	PV+ DSTATCOM +NRX
Eloss (MWh)	1.19726	1.1513	0.6680	0.5421	1.0162	0.7489	0.7242
Egrid (MWH)	27.44682	26.4059	15.3211	12.4355	23.3073	17.1766	16.6100
Optimal loc 1	-	17	-	7	15	-	2
Optimal loc 2	-	19		25	52		46
Psr1 (kW)	-	500	-	539	500	-	500
Psr2 (kW)	-	825		534	500		500
Qds1 (kVAr)	-	500	-	500	500	-	500
Qds2 (kVAr)	-	500		500	500		500
TVDev	1.24867 E+4	10852.5384	11314.4386	8278.4685	11383.8933	11059.5843	9489.7015
VSID	5.40257 E+5	559748.8951	539816.1713	552283.9652	5.51959 E+5	5.41474 E+5	5.48543 E+5
Closs ($)	7.1836199 E+4	6.9078 E+4	4.0080 E+4	3.2526 E+4	6.0972 E+4	4.4934 +4	4.3452 +4
Cgrid ($)	2.634895 E+6	2.534966 E+6	1.470825 E+6	1.193808 E+6	2.243808 E+6	1.648953 E+6	1.594560 E+6
Cpv ($)	-	1.44255 E+5	-	1.16819 E+5	1.08872 +5	0	1.08872 +5
Cds ($)	-	5.305 E+3	-	5.305 E+3	5.305 E+3	0	5.305 E+3
Ctotal ($)	2.706731 E+6	2.753604 E+6	1.510905 E+6	1.348458 +6	2.418957 E+6	1.693887 E+6	1.752718 E+6
Tie Switches	69,70,71, 72,73	69,70,71, 72,73	43,69,54, 61,18	43,69,54, 61,18	69,70,71, 72,73	44,17,58, 39,22	44,17,58, 39,22

Table 8 Simulation results for IEEE 69- bus system for single and two hybrid systems by HMPJA

Entity	Base Case	MPA			JFSA		
		PV + DSTATCOM	NRX	PV + DSTATCOM + NRX	PV + DSTATCOM	NRX	PV+ DSTATCOM +NRX
Eloss (MWh)	1.19726	1.02679	0.73328	0.68705	1.02382	0.6632	0.6306
Egrid (MWH)	27.44682	23.5502	16.8185	15.75820	23.4821	15.2126	14.4646
Optimal loc 1	-	15	-	61	11	-	2
Optimal loc 2	-		-	-	12	-	19
Psr1 (kW)	-	2571	-	1048	1000	-	700
Psr2 (kW)	-	-	-	-	1000	-	700
Qds1 (kVAr)	-	100	-	105	700	-	700
Qds2 (kVAr)	-	-		-	700	-	700
TVDev	1.24867 E+4	1.1957 E+4	1.0553 E+4	9.236 E+3	1.07 E+03	1.0291 E+4	7.016 E+3
VSID	5.40257 E+5	5.51881 E+5	5.43531 E+5	5.48883 E+5	5.57 E+05	5.43954 E+5	5.59230 E+5
Closs ($)	7.1836199 E+4	6.1566 E+4	4.3997 E+4	4.1223 E+4	6.1429 E+04	3.3979 E+4	3.7836 E+4
Cgrid ($)	2.634895E +6	2.259082 E+6	1.61457 E+5	1.557926 E+6	2.254282 E+06	1.460409 E+6	1.388860 E+6
Cpv ($)	-	2.79909 E+5	-	1.14097 E+5	2.17744 E+05	-	1.52420 E+5
Cds ($)	-	5.305 E+3	-	5.586 E+3	7.427 E+03	-	7.427 E+3
Ctotal ($)	2.706731E +6	2.550452 E+6	2.222720 E+6	2.227695 E+6	2.540882 E+06	1.800208 +6	1.586543 E+6
Tie Switches	69,70,71,7 2,73	69,70,71, 72,73	13,17,21, 42,58	13,17,21, 42,58	69,70,71, 72,73	71,54,14, 64,9	71,54,14, 64,9

Table 9 Comparative analysis for IEEE 69- bus system for single and two hybrid systems

Entity	Base Case	MPA			JFSA		
		PV + DSTATCOM	NRX	PV + DSTATCOM + NRX	PV + DSTATCOM	NRX	PV+ DSTATCOM +NRX
Eloss (MWh)	1.19726	1.02679	0.6582	1.3345	1.02382	0.8136	1.1174
Egrid (MWH)	27.44682	23.5502	24.857	26.604	23.58		21.6146
Optimal loc 1	-	15	62	57	11	63	62
Optimal loc 2	-		-		12	57	58
Psr1 (kW)	-	2571	1113	532	1000	690	1805
Psr2 (kW)	-	-	-		1000	1337	1316
Qds1 (kVAr)	-	100	1290	2689	700	1449	935
Qds2 (kVAr)	-	-	-		700	581	1683
TVDev	1.24867 E+4	1.1957 E+4	8.74E+03	7.61E+03	1.07E+03	6.95E+03	6.12E+03
VSID	5.40257 E+5	5.51881 E+5	5.62E+05	5.66E+05	5.57E+05	5.69E+05	5.77E+05
Closs ($)	7.1836199 E+4	6.1566 E+4	3.95E+04	8.01E+04	6.17E+04	4.88E+04	6.70E+04
Cgrid ($)	2.634895E +6	2.259082 E+6	2.39E+06	2.55E+06	2.26E+06	2.24E+06	2.08E+06
Cpv ($)	-	2.79909 E+5	1.21E+05	5.72E+04	1.84E+05	2.21E+05	3.40E+05
Cds ($)	-	5.305 E+3	6.84E+03	1.43E+04	7.49E+03	1.08E+04	1.39E+04
Ctotal ($)	2.706731E +6	2.550452 E+6	2.55E+06	2.71E+06	2.52E+06	2.519764E	2.50E+06

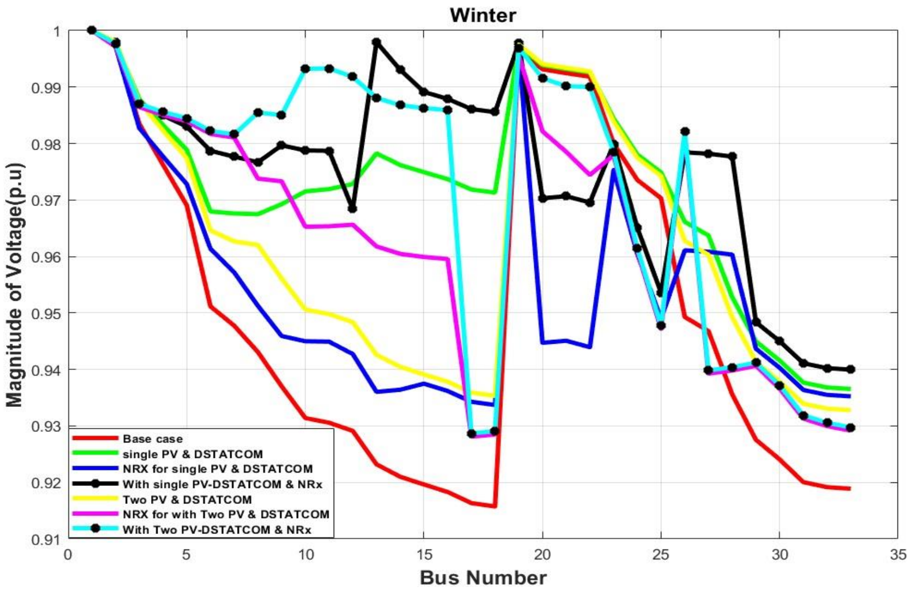

(a)

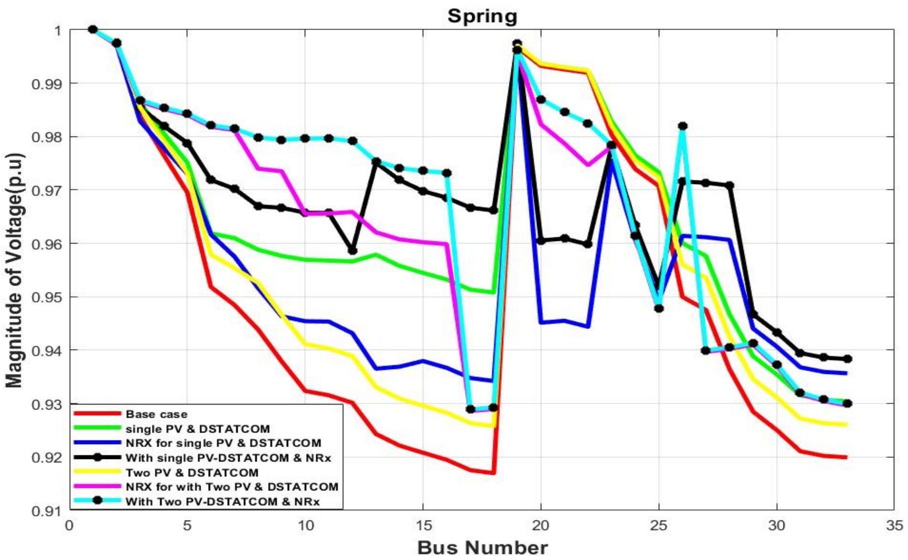

(b)

Fig. 10 VP of the 33-bus system by incorporating the one and two hybrid systems PV-DSTATCOM with NRX in (a) Winter, (b) Spring (CONTD…)

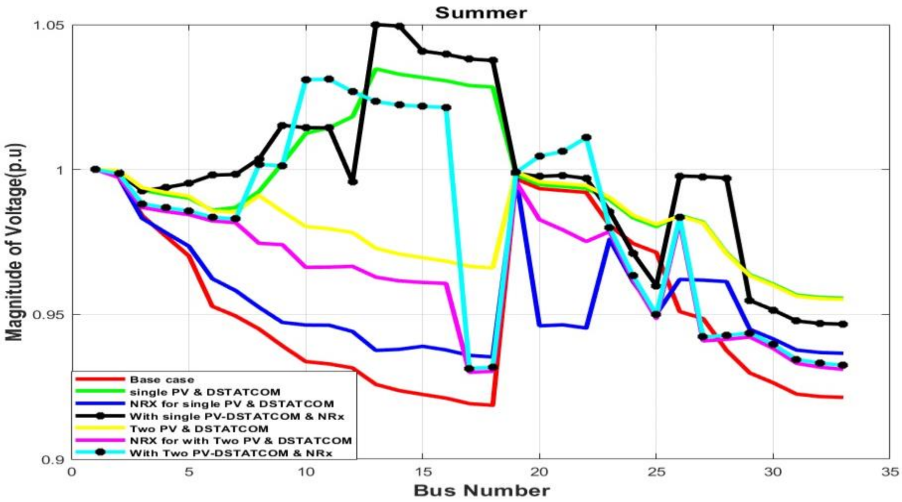

(c)

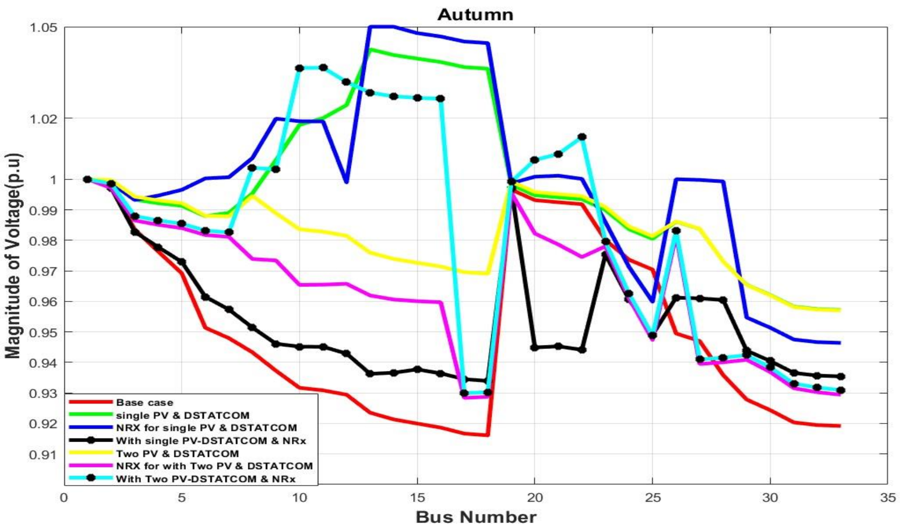

(d)

Fig. 10 VP of the 33-bus system by incorporating the one and two hybrid systems PV-DSTATCOM with NRX in (c) Summer, (d) Autumn

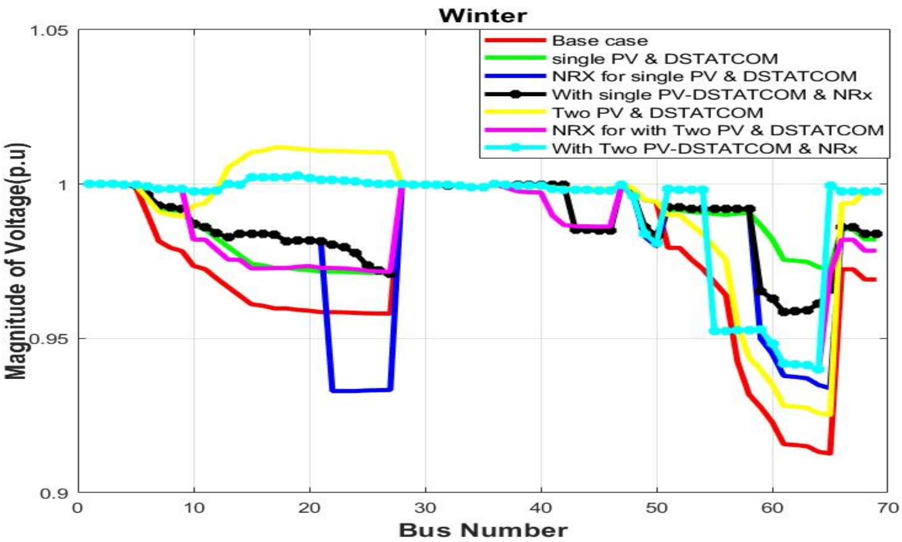

(a)

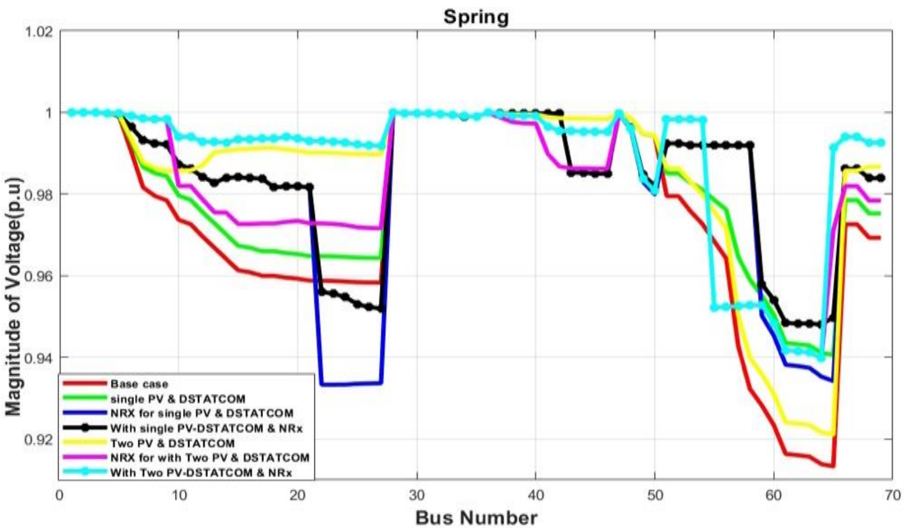

(b)

Fig. 11 VP of the 69-bus system by incorporating the one and two hybrid systems PV-DSTATCOM with NRX in (a) Winter (b) Spring (CONTD…)

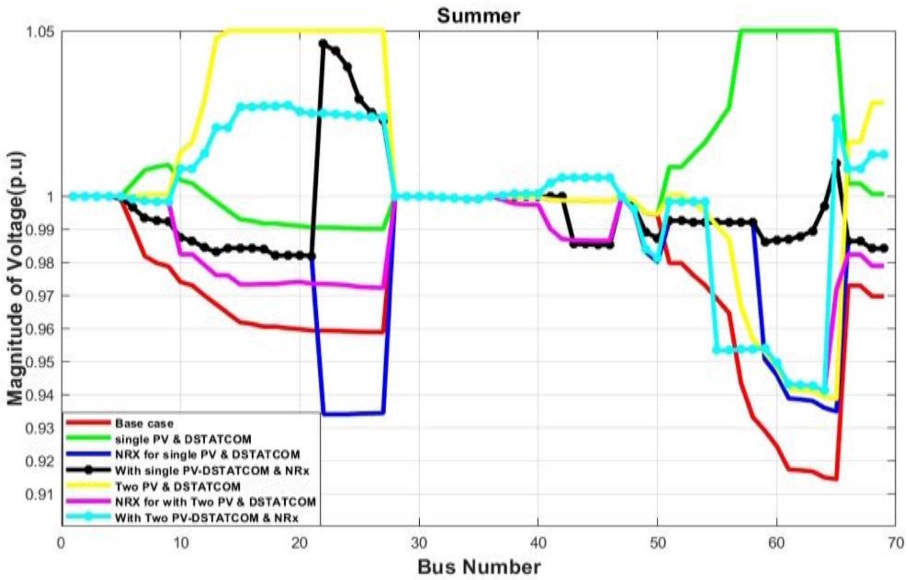

(c)

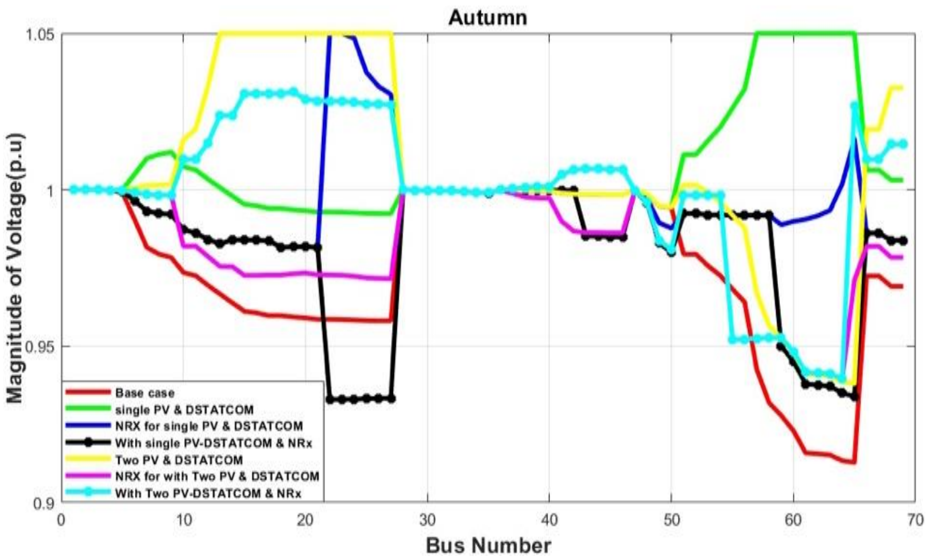

(d)

Fig. 11 VP of the 69-bus system by incorporating the one and two hybrid systems PV-DSTATCOM with NRX in (c) Summer (d) Autumn

6. CONCLUSION

This study addresses the best design and evaluation of integrating a combined system with PVDG and DSTATCOM in a reconfigured PDN while taking seasonal fluctuations in solar irradiance and load demand into account. With the use of gaussian and beta probability density functions, demand for load and solar irradiance's random nature are accurately represented. A hybrid marine predator jellyfish search algorithm (HMPJA) has been presented based on the learning automata to improve the method's dependability. This integration aims to provide a more resilient and effective optimization method that can handle a variety of difficulties in different problem scenarios. A multi-objective function's ideal location and size have been determined by applying the suggested HMPJA, which takes into account factors including cost savings, VP, and stability index enhancement in the reconfigured network. The proposed technique has been applied to IEEE 33-bus and 69-bus systems. A comparison has been made to mitigate power loss under load and solar irradiance variation to certify that the suggested technique works. The suggested HMPJA may be used as a future research project to address challenging issues related to power system optimization, such as combined economic emission dispatch, microgrid energy management, and the best location for distributed generation sources. This would aid in evaluating the algorithm robustness and effectiveness in managing a variety of complex restrictions within the allotted time.

REFERENCES

[1] M. S. Shaikh, C. Hua, M. A. Jatoi, M. M. Ansari and A. A. Qader, "Parameter Estimation of AC Transmission Line Considering Different Bundle Conductors Using Flux Linkage Technique", *IEEE Can. J. Electr. Comput. Eng.*, vol. 44, no. 3, pp. 313-320, June 2021.

[2] H. B. Tolabi, M. Gandomkar and M. B. Borujeni, "Reconfiguration and Load Balancing by Software Simulation in a Real Distribution Network for Loss Reduction", *IEEE Can. J. Elect. Electron. Eng.*, vol. 2, no. 8, pp. 386-391, Aug. 2011.

[3] R. S. Rao, Sadhu, S. V. L. N. Narasimham, M. R. Raju and A. S. Rao, "Optimal NRX of Large-Scale Distribution System Using Harmony Search Algorithm", *IEEE Trans. Power Syst.*, vol. 26, no. 3, pp. 1080-1088, Sept. 2011.

[4] A. Merlin and H. Back, "Search for a Minimal-Loss Operating Spanning Tree Configuration in an Urban Power Distribution System", In Proceedings of the 5th Power System Computation Conference (PSCC), Cambridge, U.K., vol 5, Sept. 1975, pp. 1-18.

[5] A. Kavousi-Fard and T. Niknam, "Multi-Objective Stochastic Distribution Feeder Reconfiguration from the Reliability Point of View", *Energy*, vol. 64, pp. 342-354, Jan. 2014.

[6] A. M. Helmi, R. Carli, M. Dotoli and H. S. Ramadan, "Efficient and Sustainable Reconfiguration of Distribution Networks via Metaheuristic Optimization", *IEEE Trans. Autom. Sci. Eng.*, vol. 19, no. 1, pp. 82-98, May 2021.

[7] A. O. Salau, Y. W. Gebru and D. Bitew. "Optimal NRX for Power Loss Minimization and Voltage Profile Enhancement in Distribution Systems", *Heliyon*, vol. 6, no. 6, p. e04233, June 2020.

[8] A. A. M. Raposo, A. B. Rodrigues and M. D. G. da Silva, "Robust Meter Placement for State Estimation Considering Distribution NRX for Annual Energy Loss Reduction", *Electr. Power Syst. Res.*, no. 182, p. 106233, May 2020.

[9] T. Yuvaraj, K. R. Devabalaji, N. Prabaharan, H. H. Alhelou, A. Manju, P. Pal, and P. Siano, "Optimal Integration of Capacitor and Distributed Generation in Distribution System Considering Load Variation Using Bat Optimization Algorithm", *Energies*, vol. 14, no. 12, p. 3548, June 2021.

[10] S. S. Parihar and N. Malik, "Optimal Allocation of Renewable DGs in a Radial Distribution System Based on New Voltage Stability Index", *Int. Trans. Electr. Energy Syst.*, vol. 30, no. 4, pp. 1-19, Apr. 2020.

[11] S. Saha, and V. Mukherjee, "Optimal Placement and Sizing of DGs in RDS Using Chaos Embedded SOS Algorithm", *IET Gener. Transm. Distrib.*, vol. 10, no. 14, pp. 3671-3680, Nov. 2016.

[12] M. M. Esmaeil, M. R. Narimani, M. H. Khooban and A. Azizivahed. "Multi-Objective Distribution Feeder Reconfiguration to Improve Transient Stability, and Minimize Power Loss and Operation Cost Using an Enhanced Evolutionary Algorithm at the Presence of Distributed Generations", *Int. J. Electr. Power Energy Syst.*, vol. 76, pp. 35-43, Mar. 2016.
[13] P. Guru, N. Malik, and S. Mahapatra. "The Synergy of MPJSA: a Novel Meta-Heuristic Approach for Optimizing Distribution Systems with DGs", *FU: Elec. Energ.*, vol. 37, no. 3, pp. 541-560, Oct. 2024.
[14] M. S. Shaikh, C. Hua, M. A. Jatoi, M. M. Ansari and A. A. Qader, "Application of Grey Wolf Optimisation Algorithm in Parameter Calculation of Overhead Transmission Line System", *IET Sci. Meas. Technol.*, vol. 15, no. 2, pp. 218-231, Mar. 2021.
[15] S. S. Parihar and N. Malik, "Analysing the Impact of Optimally Allocated Solar PV-based DG in Harmonics Polluted Distribution Network", *Sustain. Energy Technol. Assess.*, vol. 49, p. 101784, Feb. 2022.
[16] S. N. Dehedkar and S. Raj, "Determination of Optimal Location and Implementation of Solar Photovoltaic System Using ETAP", In Proceedings of the IEEE 2nd International Symposium on Sustainable Energy, Signal Processing and Cyber Security (ISSSC), Dec. 2022, pp. 1-4.
[17] A. R. Gupta and A. Kumar, "Deployment of Distributed Generation with DFACTS in Distribution System: A Comprehensive Analytical Review", *IETE J. Research*, vol. 68, no. 2, pp. 1195-212, July 2019.
[18] M. Ebeed, S. Kamel, S. H. A. Aleem, and A. Y. Abdelaziz, "Optimal Allocation of Compensators", *Electric Distribution Network Planning*, pp. 321-353, 2018.
[19] S. Jazebi, S. H. Hosseinian and B. Vahidi, "DSTATCOM Allocation in Distribution Networks Considering Reconfiguration Using Differential Evolution Algorithm", *Energy Convers. Manage.*, vol. 52, no. 7, pp. 2777-2783, July 2011.
[20] O. P. Mahela and A. G. Shaik, "Power Quality Improvement in Distribution Network Using DSTATCOM with Battery Energy Storage System", *Int. J. Electr. Power Energy Syst.*, vol. 83, pp. 229-240, Dec. 2016.
[21] S. S. Parihar and N. Malik, "Network Reconfiguration in the Presence of Optimally Integrated Multiple Distributed Generation Units in a Radial Distribution Network", *Eng. Optim.*, vol. 56, no. 5, pp. 679-99, May 2024.
[22] S. A. Taher, and S. A. Afsari, "Optimal Location and Sizing of DSTATCOM in Distribution Systems by Immune Algorithm", *Int. J. Electr. Power Energy Syst.*, vol. 60, pp. 34-44, Sept. 2014.
[23] T. Yuvaraj, K. R. Devabalaji and K. Ravi, "Optimal Placement and Sizing of DSTATCOM Using Harmony Search Algorithm", *Energy Procedia*, vol. 79, pp. 759-765, Nov. 2015.
[24] N. Salman, A. Mohamed and H. Shareef, "Reliability Improvement in Distribution Systems by Optimal Placement of DSTATCOM Using Binary Gravitational Search Algorithm", Przegląd Elektrotechniczny, vol. 88, no. 2, pp. 295-299, Jan. 2012.
[25] M. Sedighizadeh and A. E. Moarref, "The Imperialist Competitive Algorithm for Optimal Multi-Objective Location and Sizing of DSTATCOM in Distribution Systems Considering Loads Uncertainty", *INAE Lett. 2*, pp. 83-95, Sept. 2017.
[26] M. S. Shaikh, S. Raj, R. Babu, S. Kumar and K. Sagrolikar, "A Hybrid Moth–Flame Algorithm with Particle Swarm Optimization with Application in Power Transmission and Distribution", *Decis. Anal. J.*, vol. 6, p. 100182, Mar. 2023.
[27] M. S. Shaikh, S. Raj, S. A. Latif, W. F. M. and S. Kamel, "Optimizing Transmission Line Parameter Estimation with Hybrid Evolutionary Techniques", *IET Gener. Transm. Distrib.*, vol. 18, no. 9, pp. 1795-1814, May 2024.
[28] H. B. Tolabi, M. H. Ali and M. Rizwan, "Simultaneous Reconfiguration, Optimal Placement of DSTATCOM, and Photovoltaic Array in a Distribution System Based on Fuzzy-ACO Approach", *IEEE Trans. Sustain. Energy*, vol. 6, no. 1, pp. 210-218, Jan. 2015.
[29] K. R. Devabalaji and K. Ravi, "Optimal Size and Siting of Multiple DG and DSTATCOM in Radial Distribution System Using Bacterial Foraging Optimization Algorithm", *Ain Shams Eng. J.*, vol. 7, no. 3, pp. 959-971, Sept. 2016.
[30] S. Devi and M. Geethanjali, "Optimal Location and Sizing Determination of Distributed Generation and DSTATCOM Using Particle Swarm Optimization Algorithm", *Int. J. Electr. Power Energy Syst.*, vol. 62, pp. 562-570, Nov. 2014.
[31] T. Yuvaraj, K. R. Devabalaji, and S. B. Thanikanti, "Simultaneous Allocation of DG and DSTATCOM Using Whale Optimization Algorithm", *Iranian J. Sci. Technol. Trans. Electr. Eng.*, vol. 44, no. 2, pp. 879-896, June 2020.
[32] S. Raj, B. Bhattacharyya "Optimal Placement of TCSC and SVC for Reactive Power Planning Using Whale Optimization Algorithm", *Swarm Evol. Comput.*, vol. 40, pp. 131-143, June 2018.
[33] Y. Thangaraj and R. Kuppan, "Multi-Objective Simultaneous Placement of DG and DSTATCOM Using Novel Lightning Search Algorithm", *J. Appl. Res. Technol.*, vol. 15, no. 5, pp. 477-491, Oct. 2017.

[34] S. G. R. Chinnaraj and R. Kuppan, "Optimal Sizing and Placement of Multiple Renewable Distribution Generation and DSTATCOM in Radial Distribution Systems Using Hybrid Lightning Search Algorithm-Simplex Method Optimization Algorithm",' Computat. Intell., vol. 37, no. 4, pp. 1673-1690, Nov. 2021.
[35] S. R. Ghatak, S. Sannigrahi and P. Acharjee, "Optimised Planning of Distribution Network with Photovoltaic System, Battery Storage, and DSTATCOM", *IET Renew. Power Gener.*, vol. 12, no. 15, pp. 1823-1832, Nov. 2018.
[36] A. Selim, S. Kamel, A. S. Alghamdi and F. Jurado, "Optimal Placement of DGs in Distribution System Using an Improved Harris Hawks Optimizer Based on Single- and Multi-Objective Approaches", *IEEE Access*, vol. 8, pp. 52815-52829, Mar. 2020.
[37] S. S. Parihar and N. Malik, "Possibilistic Uncertainty Assessment in the Presence of Optimally Integrated Solar PVDG and Probabilistic Load Model in Distribution Network", *Facta Universitatis Series Electronics and Energetics*, vol. 35, no. 1, pp. 71-92, Mar. 2022.
[38] H. M. Zawbaa, E. Emary and C. Grosan, "Feature Selection via Chaotic Antlion Optimization", *PLoS ONE*, vol. 11, no. 3, p. e0150652, Mar. 2016.
[39] E. S. Oda, A. M. A. E. Hamed, A. A. Elbaset, M. A. E. Sattar and M. Ebeed, "Stochastic Optimal Planning of Distribution System Considering Integrated Photovoltaic-Based DG and DSTATCOM Under Uncertainties of Loads and Solar Irradiance", *IEEE Access*, vol. 9, pp. 26541-26555, Feb. 2021.
[40] Q. Sun, R. Han, H. Zhang, J. Zhou and J. M. Guerrero, "A Multiagentbased Consensus Algorithm for Distributed Coordinated Control of Distributed Generators in the Energy Internet", *IEEE Trans. Smart Grid*, vol. 6, no. 6, pp. 3006-3019, Nov. 2015.
[41] M. Ebeed, A. Ali, M. I. Mosaad, and S. Kamel, "An Improved Lightning Attachment Procedure Optimizer for Optimal Reactive Power Dispatch with Uncertainty in Renewable Energy Resources", *IEEE Access*, vol. 8, pp. 168721-168731, 2020.
[42] R. H. A. Zubo, G. Mokryani and R. Abd-Alhameed, "Optimal Operation of Distribution Networks with High Penetration of Wind and Solar Power within a Joint Active and Reactive Distribution Market Environment", *Appl. Energy*, vol. 220, pp. 713-722, June 2018.
[43] A. Faramarzi, M. Heidarinejad, S. M. Mirjalili and A. H. Gandomi, "Marine Predators Algorithm: A Nature-Inspired Metaheuristic", *Expert Syst. Appl.*, vol. 152, p. 113377, August 2020.
[44] J. S. Chou and D. N Truong, "A Novel Metaheuristic Optimizer Inspired by Behavior of Jellyfish in Ocean", *Appl. Math. Comput.*, vol. 389, p. 125535, Jan. 2021.
[45] S. Kamel, A. Selim, W. Ahmed, F. Jurado, "Single-and Multi-Objective Optimization for Photovoltaic Distributed Generators Implementation in Probabilistic Power Flow Algorithm", *Electr. Eng.,* vol. 102, no. 1, pp. 331-347, Mar. 2020.
[46] E. S. Ali, S. M. A. Elazim, A. Y. Abdelaziz, "Ant Lion Optimization Algorithm for Optimal Location and Sizing of Renewable Distributed Generations", *Renew. Energy*, vol. 101, pp. 1311-1324, Feb. 2017.